Quasinormal modes of a Schwarzschild black hole immersed in an electromagnetic universe

Ali Övgün[1,2,3;1)]   İzzet Sakallı[2;2)]   Joel Saavedra[1;3)]

[1] Instituto de Física, Pontificia Universidad Católica de Valparaí so, Casilla 4950, Valparaíso, Chile.
[2] Physics Department, Arts and Sciences Faculty, Eastern Mediterranean University, Famagusta, North Cyprus via Mersin 10, Turkey
[3] School of Natural Sciences, Institute for Advanced Study, 1 Einstein Drive, Princeton, NJ 08540, USA

Abstract: We study the quasinormal modes (QNMs) of a Schwarzschild black hole immersed in an electromagnetic (EM) universe. The immersed Schwarzschild black hole (ISBH) originates from the metric of colliding EM waves with double polarization [Class. Quantum Grav. 12, 3013 (1995)]. The perturbation equations of the scalar fields for the ISBH geometry are written in the form of separable equations. We show that these equations can be transformed to the confluent Heun's equations, for which we are able to use known techniques to perform analytical quasinormal (QNM) analysis of the solutions. Furthermore, we employ numerical methods (Mashhoon and 6th-order Wentzel-Kramers-Brillouin (WKB)) to derive the QNMs. The results obtained are discussed and depicted with the appropriate plots.

Keywords: quasinormal modes, scalar particles, Schwarzschild, electromagnetic universe, wave scattering, heun functions

PACS: 04.20.Jb, 04.62.+v, 04.70.Dy   **DOI:** 10.1088/1674-1137/42/10/105102

1   Introduction

Classical black holes are closed systems that do not emit any signal to an outside observer. The only way to obtain information from a black hole is to study its relativistic wave dynamics with quantum mechanics, e.g., Hawking radiation, quasinormal modes (QNMs), and gravitational waves. To have QNMs, a black hole must be perturbed. A fair analogy to this concept is the ringing of a bell, which is a damped harmonic oscillator. The perturbation of a black hole has at least three stages: (i) the transient stage, which depends on the initial perturbation; (ii) the QNM ring-down, which is an important stage that reveals unique frequencies containing information about the source; and (iii) the exponential/power-law tail, which occurs when the energy is very low at the end of the perturbation. QNMs can be found by applying perturbations to the black hole spacetime with appropriate boundary conditions: the wave solution should be purely outgoing at infinity and purely ingoing at the event horizon [1–4, 19]. For reviews and research papers on QNMs, the reader may refer to Refs. [5–12]. The detection of gravitational waves [13–15] has brought QNMs into the spotlight again. However, the QNMs (having frequencies above 500 Hz [16]) of lower mass black holes

and neutron star mergers are presently not detectable. The main problem is the increasing quantum shot noise [17] in the high frequency regime. However, recent developments [18] are very promising for the detection of QNMs in the near future.

Our main aim in this study is to study the QNMs of massive/massless scalar fields in immersed Schwarzschild black hole (ISBH) spacetime. To this end, we shall use particular analytical and numerical methods. Iyer and Will [20] were the first researchers to obtain QNMs with the help of the third order WKB approximation. Later on, their study was extended to the sixth order by Konoplya and Zhidenko [21–23]. The WKB approximations have also been considered by other researchers to compute the QNMs of various spacetimes [24–51].

The ISBH solution is given by [52–54]:

$$ds^2 = -F(r)dt^2 + \frac{1}{F(r)}dr^2 + r^2(d\theta^2 + \sin(\theta)^2 d\varphi^2), \quad (1)$$

where

$$F(r) = 1 - \frac{2M}{r} + \frac{M^2(1-a^2)}{r^2}, \quad (2)$$

in which M denotes the mass-parameter and a is the interpolation parameter [54, 55]: $1 \geq a \geq 0$. Letting the effective charge be $Q_{\text{eff}} \equiv M^2(1-a^2)$, it is clear that

when $a=1$ i.e., $Q_{\text{eff}}=0$, metric (1) is nothing but the Schwarzschild black hole. However, the case of $a=0$ ($Q_{\text{eff}}=M^2$) corresponds to the Reissner-Nordström black hole [56, 57]. The metric function $F(r)$ can be rewritten as

$$F(r)=\frac{(r-r_p)(r-r_n)}{r^2}, \tag{3}$$

where $r_p=M(1+a)$ and $r_n=M(1-a)$ are the event and inner horizons, respectively. To illustrate the effect of the a-parameter on the EM structure of the spacetime, one can use the Newman-Penrose formalism [58]. To this end, the null tetrad frame $(l,n,m,\overline{m})$, which satisfies the orthogonality conditions ($l.n=-m.\overline{m}=1$) is chosen to be

$$l_\mu=\mathrm{d}t-\frac{\mathrm{d}r}{F(r)},$$

$$2n_\mu=F(r)\mathrm{d}t+\mathrm{d}r,$$

$$\sqrt{2}m_\mu=-r(\mathrm{d}\theta+\mathrm{i}\sin\theta\mathrm{d}\phi),$$

$$\sqrt{2}\overline{m}_\mu=-r(\mathrm{d}\theta-\mathrm{i}\sin\theta\mathrm{d}\phi). \tag{4}$$

Thus, the non-zero Weyl and Ricci scalars can be computed as follows:

$$\Psi_2=-\frac{(r_p+r_n)r-2r_pr_n}{2r^4}=-\frac{1}{r^4}[Mr+Q_{\text{eff}})], \tag{5}$$

$$\Phi_{11}=\frac{r_pr_n}{2r^4}=\frac{Q_{\text{eff}}}{2r^4}. \tag{6}$$

Since the only non-zero Weyl scalar is Eq. (5), the metric (1) represents a Petrov type-D [xx] spacetime. The effect of the a-parameter on the gravitational and EM fields is now clearer:

$$\text{Gravity}\rightarrow(a=1)\rightarrow\Psi_2=\frac{-M}{r^3},\ \Phi_{11}=0.$$

$$\text{Gravity+EM}\rightarrow(0\leq a<1)\rightarrow\Psi_2\neq0\neq\Phi_{11}.$$

The Hawking temperature [59] is expressed in terms of the surface gravity (κ) as $T_H=\frac{\kappa}{2\pi}$. For the ISBH geometry, it is given by

$$T_H=\frac{\kappa}{2\pi}=\frac{F'(r)}{4\pi}\bigg|_{r=r_p}=\frac{a}{2M\pi(a+1)^2}. \tag{7}$$

This paper is organized as follows. In Section 2, we provide a complete analytical solution to the massive Klein-Gordon equation (KGE) in terms of the confluent Heun functions. We then show how the QNMs can be computed from that obtained exact solution. Sections 3 and 4 are devoted to numerical studies of the massless KGE in the ISBH geometry. We obtain the corresponding effective potential and analyze it. We present two numerical methods (the Mashhoon and the sixth-order WKB) for computing the QNMs of the ISBH. Finally, we summarize our discussions in the conclusion.

2   Analytical QNMs

Let us consider a massive scalar field that obeys the KGE on the ISBH metric (1). Recall that a massive KGE is given by (e.g., Ref. [60])

$$\frac{1}{\sqrt{-g}}\partial_\alpha\left(\sqrt{-g}g^{\alpha\beta}\partial_\beta\Psi_0\right)-\mu_0^2\Psi_0=0. \tag{8}$$

Here, μ_0 and Ψ_0 represent the mass and the scalar field, respectively. It is straightforward to see that Eq. (8) is separable with the following ansatz:

$$\Psi_0=\Psi_0(\boldsymbol{r},t)=\mathcal{R}(r)\mathcal{A}(\theta)\mathrm{e}^{\mathrm{i}m\varphi}\mathrm{e}^{-\mathrm{i}\omega t}, \tag{9}$$

where ω denotes the frequency of the wave and m denotes the magnetic quantum number associated with the rotation in the φ direction. By defining an eigenvalue (λ), one can show that Eq. (8) leads to the following angular and radial equations:

$$\sin(\theta)\frac{\mathrm{d}^2}{\mathrm{d}\theta^2}\mathcal{A}(\theta)+\left(\frac{\mathrm{d}}{\mathrm{d}\theta}\mathcal{A}(\theta)\right)\cos(\theta)$$

$$+\left(\lambda\sin(\theta)-\frac{m^2}{\sin(\theta)}\right)\mathcal{A}(\theta)=0, \tag{10}$$

and

$$\left(\frac{\mathrm{d}}{\mathrm{d}r}\Delta(r)\right)\frac{\mathrm{d}}{\mathrm{d}r}\mathcal{R}(r)+\Delta(r)\frac{\mathrm{d}^2}{\mathrm{d}r^2}\mathcal{R}(r)$$

$$+\left(\frac{r^4\omega^2}{\Delta(r)}-\lambda-\mu_0^2r^2\right)\mathcal{R}(r)=0. \tag{11}$$

The solution of the angular equation (10) is given in terms of the four-dimensional spheroidal functions [61]. To obtain the exact solution of the radial equation (11), we first introduce a new variable:

$$z=(r-r_p)\Bbbk_m^{-1}, \tag{12}$$

where $\Bbbk_m=r_p-r_n$. By using Eq. (12) in Eq. (11), one can transform the radial equation into the following form:

$$z(1-z)\frac{\mathrm{d}^2}{\mathrm{d}z^2}\mathcal{R}(z)+(1-2z)\frac{\mathrm{d}}{\mathrm{d}z}\mathcal{R}(z)$$

$$+\left(\lambda+\mu_0^2(r_p-\Bbbk_mz)^2-\frac{(r_p-\Bbbk_mz)^4\omega^2}{z(z-1)\Bbbk_m^2}\right)\mathcal{R}(z)=0. \tag{13}$$

Furthermore, applying a particular s-homotopic transformation [62] to $\mathcal{R}(z)$:

$$\mathcal{R}(z)=\mathrm{e}^{B_1z}z^{B_2}(1-z)^{B_3}\mathcal{U}(z), \tag{14}$$

where the coefficients B_1, B_2, and B_3 are given by

$$B_1=\Bbbk_m\sqrt{\mu_0^2-\omega^2}, \tag{15}$$

$$B_2=\frac{\mathrm{i}r_p^2\omega}{\Bbbk_m}, \tag{16}$$

$$B_3=\frac{\mathrm{i}r_n^2\omega}{\Bbbk_m}, \tag{17}$$

we obtain a differential equation for $\mathcal{U}(z)$, which is identical to the confluent Heun differential equation [63–70] (for one of the most detailed works about the applications of the Heun differential equation, the reader is referred to Ref. [71]):

$$\frac{\mathrm{d}^2}{\mathrm{d}z^2}\mathcal{U}(z)+\left(\widetilde{a}+\frac{1+\widetilde{b}}{z}-\frac{1+\widetilde{c}}{1-z}\right)\frac{\mathrm{d}}{\mathrm{d}z}\mathcal{U}(z)+\left(\frac{\widetilde{f}}{z}-\frac{\widetilde{g}}{1-z}\right)\mathcal{U}(z)=0.$$
(18)

The three parameters seen in the coefficient bracket of $\frac{d}{dz}\mathcal{U}(z)$ are given by

$$\widetilde{a}=2B_1,\ \ \widetilde{b}=2B_2,\ \ \widetilde{c}=2B_3.$$
(19)

Setting

$$\widetilde{d}=-\mathbb{k}_m\mathbb{k}_p\left(\mu_0^2-2\omega^2\right),$$
(20)

$$\widetilde{e}=\frac{-r_p^2\left[(\mu_0\mathbb{k}_m)^2-2r_p\omega^2(\mathbb{k}_m-r_n)\right]-\mathbb{k}_m^2\lambda}{\mathbb{k}_m^2},$$
(21)

where $\mathbb{k}_p=r_p+r_n$, one can also find the other two parameters of Eq. (18) as follows:

$$\widetilde{f}=\frac{1}{2}(\widetilde{a}-\widetilde{b}-\widetilde{c}+\widetilde{a}\widetilde{b}-\widetilde{b}\widetilde{c})-\widetilde{e},$$
(22)

$$\widetilde{g}=\frac{1}{2}(\widetilde{a}+\widetilde{b}+\widetilde{c}+\widetilde{a}\widetilde{c}+\widetilde{b}\widetilde{c})+\widetilde{d}+\widetilde{e}.$$
(23)

The general solution of the confluent Heun differential equation (18) is given by Ref. [72] as follows:

$$\mathcal{U}(z)=c_1\mathrm{HeunC}(\widetilde{a},\widetilde{b},\widetilde{c},\widetilde{d},\widetilde{e};z)+c_2z^{-\widetilde{b}}\mathrm{HeunC}(\widetilde{a},-\widetilde{b},\widetilde{c},\widetilde{d},\widetilde{e};z),$$
(24)

where c_1 and c_2 are integration constants. Thus, the general solution of Eq. (13) in the exterior region of the event horizon ($0\leqslant z<\infty$) reads

$$\mathcal{R}(z)=\mathrm{e}^{B_1z}(1-z)^{B_3}\Big[C_1z^{B_2}\mathrm{HeunC}(\widetilde{a},\widetilde{b},\widetilde{c},\widetilde{d},\widetilde{e};z)$$

$$+C_2z^{-B_2}\mathrm{HeunC}(\widetilde{a},-\widetilde{b},\widetilde{c},\widetilde{d},\widetilde{e};z)\Big].$$
(25)

Now, we follow one of the recent techniques [66, 70, 73] to compute the QNMs of scalar waves propagating in the geometry of an ISBH. QNMs are the solutions associated with complex frequencies. In particular, the imaginary component of the frequency states how fast the oscillation will fade over time [75].

The QNMs can be obtained from the radial solution (25) under certain boundary conditions: the Heun functions should be well-behaved at spatial infinity and finite on the horizon. This requires $\mathcal{R}(z)$ to take the form of Heun's polynomials [76], which is possible with the $\widetilde{\delta}_n$ condition [70, 73, 74]

$$\frac{\widetilde{d}}{\widetilde{a}}+\frac{\widetilde{b}+\widetilde{c}}{2}+1=-n,\qquad\text{with}\quad n=0,1,2,\dots$$
(26)

In Ref. [66], it is shown that the Heun's polynomials arising from Eq. (26) yield the most general class of solutions to the Teukolsky master equation pertinent to the

Teukolsky-Starobinsky identities [77], which are closely related to the subject of QNMs [78, 79]. Using Eq. (26), we find out that, assuming $\omega\geqslant\mu_0$,

$$i\left[\frac{-\mathbb{k}_p(2\omega^2-\mu_0^2)}{2\sqrt{\omega^2-\mu_0^2}}+\frac{\omega\left(r_p^2+r_n^2\right)}{\mathbb{k}_m}\right]+1=-n.$$
(27)

With the aid of a mathematical computer package like Maple 18 [72], one can obtain a solution for ω from Eq. (27). However, the solution is excessively lengthy, which prevents us from typing it here. On the other hand, if one considers the very light spin-0 particles with $\mu_0\sim0$, the $\widetilde{\delta}_n$ condition (26) results in

$$\frac{2\mathrm{i}\omega r_p^2}{\mathbb{k}_m}+1=-n.$$
(28)

The above equation allows the following solution for the QNMs:

$$\omega_n=\mathrm{i}\frac{\mathbb{k}_m}{2r_p^2}(n+1).$$
(29)

Recalling the definition of surface gravity (κ) from Eq. (7), we have

$$\kappa=\frac{\mathbb{k}_m}{2r_p^2}.$$
(30)

This changes Eq. (29) to the following form:

$$\omega_n=\mathrm{i}\kappa(n+1)=\mathrm{i}2\pi T_H(n+1).$$
(31)

It is obvious from Eq. (31) that an ISBH admits purely imaginary QNMs, which is in good agreement with the QNM result for a Schwarzschild black hole with a global monopole [74]. Furthermore, although it is valid for $n\to\infty$, the QNM result of Hod [80] (see also Ref. [81]), which was obtained analytically by the continued-fraction argument method [82], also supports our result (31).

3 QNMs by the Mashhoon method: Approximation with Poschl-Teller potential

As we have learned from the previous section, the mass does not play an important role in the QNMs. We therefore consider the following massless KGE to perform numerical analysis in this section:

$$\nabla^2\Phi=0.$$
(32)

We take the ansatz of the scalar field, which can be decomposed into its partial modes in terms of the spherical harmonics $Y_{l,m}(\theta,\varphi)$,

$$\Phi(r,\theta,\phi,t)=\frac{R(r)}{r}Y_{lm}(\theta,\phi)\mathrm{e}^{-\mathrm{i}\omega t}.$$
(33)

Here, ω, l, and m are the oscillating frequency of the scalar field, the angular quantum number, and the magnetic quantum number, respectively. Then, we separate

the massless KGE to obtain the following radial differential equation:

$$R'' + (\omega^2 - V_0(r))R = 0, \qquad (34)$$

where the effective potential is given by

$$V_0(r) = F(r)\left[\frac{l(l+1)}{r^2} + \frac{F'}{r}\right]. \qquad (35)$$

Note that a prime stands for the derivative with respect to the tortoise coordinates (r_*), $\mathrm{d}r_* = \frac{\mathrm{d}r}{F(r)}$. First, we investigate the features of the potential by plotting it with different values of parameters such as M and a. In Fig. 1, the potential is plotted for various values of a. It is obvious that when a increases, the height decreases.
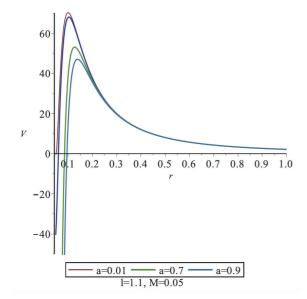

Fig. 1.   (color online) V vs. r for massless particles.

Now, we use the Mashhoon method to calculate the QNMs numerically [83–85]. Wave functions vanish at the boundaries and the QNM problem becomes a bound-states problem with a potential of $V_0 \to -V_0$. Moreover, analytic solutions of the wave equation for this kind of potential resemble the Poschl-Teller (PT) potential

$$V_{\mathrm{PT}} = \frac{V_{0_{\max}}}{\cosh^2 \alpha(r_* - r)}. \qquad (36)$$

Here, $V_{0_{\max}}$ is the effective potential (35) at the maximum point, which gives the height. The bound states of the PT potential are portrayed as follows:

$$\omega(\alpha) = W(\alpha'), \qquad (37)$$

$$W = \alpha'\left[-(n+\tfrac{1}{2}) + \frac{1}{4} + \sqrt{\frac{V_{0_{\max}}}{\alpha'^2}}\right]. \qquad (38)$$

The QNMs (ω) are calculated using the inverse of the PT potential bound states $(\alpha' = i\alpha)$. Thus, we have [83, 84]

$$\omega = \pm\sqrt{V_{0_{\max}} - \tfrac{1}{4}ff^2} - i\alpha\left(n+\tfrac{1}{2}\right), \qquad (39)$$

where n is the overtone number, and ω is calculated for varying values of n: $(-1.5, i0.3230265022)$, $(-3.0, i0.9243084555)$, $(-7.5, i2.470697496)$, and $(-15.0, i4.985413335)$. It is clear that the field decays faster for large values of a. From the above solution it is seen that the perturbations are stable $(\Im\omega < 0)$ as well as that the damping increases with the overtone number n.

4   Numerical results with the sixth-order WKB method

In this section, by employing Konoplya's sixth order WKB approach [21], we compute the QNM frequencies and obtain the QNMs from the following identity:

$$\frac{\omega^2 - V_0}{\sqrt{-2V_0''}} - L_2 - L_3 - L_4 - L_5 - L_6 = \left(n + \tfrac{1}{2}\right). \qquad (40)$$

Here, $V_{0_{\max}}''$ is the second derivative of the maximum effective potential. Details of the expressions for L_i can be found in Ref. [21], and n is the overtone number. The last value is the maximum point of the potential.

Table 1. $a = 0.1$.

l	ω_1	ω_2	ω_3	ω_4	ω_5	ω_6
1	0.376627-i0.089963	0.376291-i0.0900433	0.376188-i0.0896098	0.374267-i0.0900696	0.376185-i0.0977338	0.4041-i0.0909823
2	0.623756-i0.08954	0.623774-i0.0895374	0.623761-i0.0894481	0.623273-i0.0895182	0.623696-i0.0924193	0.640826-i0.0899488
3	0.872001-i0.0893856	0.872008-i0.0893849	0.872006-i0.089359	0.871821-i0.089378	0.871975-i0.0908726	0.884262-i0.0896099
4	1.12049-i0.0893221	1.12049-i0.089322	1.12049-i0.0893121	1.1204-i0.0893192	1.12047-i0.0902263	1.13004-i0.0894622

Table 2. $a = 0.5$.

l	ω_1	ω_2	ω_3	ω_4	ω_5	ω_6
1	0.345998-i0.0981664	0.34612-i0.0981318	0.346002-i0.0977128	0.344377 - i0.0981738	0.346651-i0.105874	0.377539-i0.0972126
2	0.570878-i0.0975128	0.5709-i0.097509	0.570887-i0.0974313	0.570478-i0.097501	0.570995-i0.100477	0.590496-i0.0971589
3	0.797048-i0.0973316	0.797053-i0.097331	0.79705-i0.0973092	0.796896-i0.097328	0.797086-i0.0988706	0.811203-i0.0971499
4	1.02363-i0.0972581	1.02363-i0.0972579	1.02363-i0.0972497	1.02355-i0.0972567	1.02364-i0.0981953	1.03468-i0.0971477

Table 3. a=0.9.

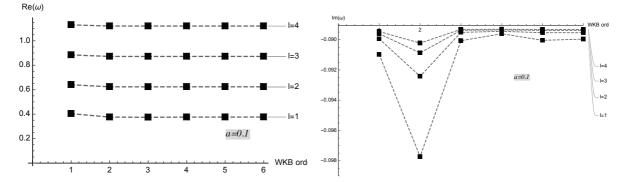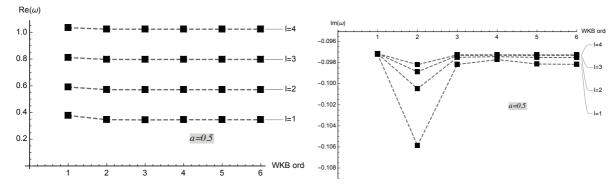| l	ω_1	ω_2	ω_3	ω_4	ω_5	ω_6
1	0.303024-i0.0986391	0.303153-i0.0985971	0.303055-i0.0982969	0.301332-i0.0988591	0.338945-i0.0971429	0.338945-i0.0971429
2	0.500192-i0.097696	0.500207-i0.097693	0.500198-i0.0976455	0.499781-i0.097727	0.500499-i0.101335	0.522507-i0.097067
3	0.698423-i0.0974405	0.698426-i0.0974402	0.698424-i0.097428	0.698269-i0.0974496	0.698533-i0.0993224	0.714528-i0.0970991
4	0.897001-i0.097336	0.897002-i0.0973359	0.897001-i0.0973315	0.896928-i0.0973395	0.897052-i0.0984799	0.909582-i0.0971233

Fig. 2.   The real and imaginary part of QNMs with sixth-, fifth-, fourth-, third-, and second-order WKB formula and the eikonal approximation for a=0.1, M=1 and s=0 mode with the multipole numbers l=(1,2,3,4).

Fig. 3.   The real and imaginary part of QNMs with sixth-, fifth-, fourth-, third-, and second-order WKB formula and the eikonal approximation for a=0.5, M=1 and s=0 mode with the multipole numbers l=(1,2,3,4).
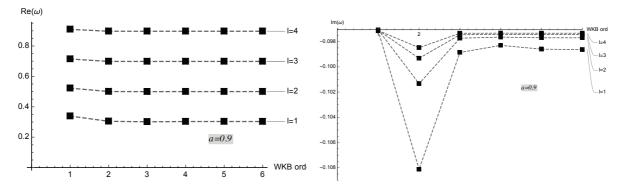

Fig. 4.   The real and imaginary part of QNMs with sixth-, fifth-, fourth-, third-, and second-order WKB formula and the eikonal approximation for a=0.9, M=1 and s=0 mode with the multipole numbers l=(1,2,3,4).
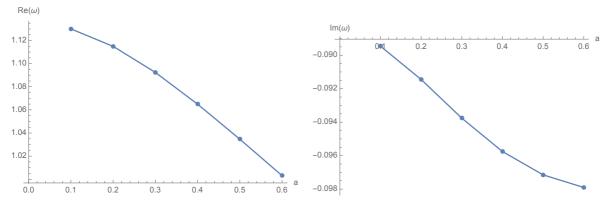
Fig. 5.   (color online) The real and imaginary part of QNMs with sixth-order WKB formula for a versus $\text{Re}(\omega)$ and a versus $\text{Im}(\omega)$ for $M=1$, $s=0$ mode with the multipole number $l=4$.

The QNM frequencies are given by $\omega = \omega_R - i\omega_I$. A positive imaginary value of $i\omega_I$ means that it is damped and negative $i\omega_I$ means that there is an instability.

The result of Eq. (40) gives the list of QNMs found with sixth-, fifth-, fourth-, third-, and second-order WKB expressions and the eikonal approximations with different values of multipole number $l = 1,2,3,4$ and $a=0.1,0.5,0.9$.

The convergence of the WKB formula for varying values of a and the expedited field decay can be seen in Tables 1, 2, 3 and is plotted in Figs. 2, 3, 4 for values of $a=(0.1,0.5,0.9)$, $M=1$ and $s=0$ mode with the multipole numbers $l=(1,2,3,4)$.

5   Conclusion

In this paper, we have analytically studied massive scalar field perturbations by using the KGE in an ISBH geometry. After finding the exact solution of the radial wave equation, we have found close agreement with the obtained QNMs of the ISBH and previous studies [80–82], which were on QNMs of Schwarzschild black holes.

We then employed the sixth-order WKB approximation method to compute the QNMs. Special attention has been paid to the details of how QNMs vary with the interpolation parameter a. The plots of the QNM frequencies ω versus a show that the real part of the QNM frequency $\text{Re}\omega$ decreases with a, similarly to the imaginary part of the QNM frequency $\text{Im}\omega$ decreasing with it as shown in Fig. 5. We have also inferred from the associated graphs that if one plots the QNM frequencies from the lower to the higher overtones, taking into ac-

count different WKB orders, the comparative accuracy gets better when $l < n$. Namely, similar to the study of QNMs of test fields around regular black holes [86], the results Tables 1, 2, 3 and Figs. 2, 3, 4, 5 have shown that an increase of Q_{eff} (i.e, $a \to 0$) implies a monotonic increase of $\text{Re}\omega$ and $\text{Im}\omega$ (and vice versa): the damping rate of the wave decreases with increasing Q_{eff}. One can infer from the latter results that ISBH oscillators are "better" (more slowly damped) than the Schwarzschild BH. On the other hand, our results are contrary to the QNM results obtained for black holes in the braneworld, for which the real oscillations decrease while the damping rate increases with increasing tidal charge parameter [87].

We plan to extend our study to a rotating ISBH [54] in the near future. Moreover, in addition to the scalar perturbations, we aim to study the Dirac and Proca perturbations and quantum tunneling processes of the ISBH. The QNM frequencies of the ISBH in the eikonal limit ($l \gg 1$) by using the parameters of null geodesics [88–90] are also in our work agenda.

References

1 S. Fernando, Phys. Rev. D, **79**: 124026 (2009)
2 I. Sakalli, Int. J. Mod. Phys. A, **26**: 2263-2269 (2011); Int. J. Mod. Phys. A, **28**: 1392002 (2013)
3 D. Du, B. Wang, and R. Su, Phys. Rev. D, **70**: 064024 (2004)
4 C. Chirenti, Braz. J. Phys., **48**(1): 102 (2018)
5 K. D. Kokkotas and B. G. Schmidt, Living Rev. Rel., **2**: 2

(1999), arXiv:gr-qc/9909058

6   H-P Nollert, Class. Quantum Grav., **16**: R159 (1999)
7   E. Berti, V. Cardoso, and A. O. Starinets, Class. Quantum Grav., **26**: 163001 (2009)
8   A. Flachi and J. P. S. Lemos, Phys. Rev. D, **87**: 024034 (2013)
9   A. Nagar and L. Rezzolla, Class. Quantum Grav., **22**: R167 (2005)
10 C. B. M. H. Chirenti and L. Rezzolla, Class. Quantum Grav., **24**: 4191 (2007)
11 B. Toshmatov, C. Bambi, B. Ahmedov, Z. Stuchlik, and J. Schee, Phys. Rev. D, **96**: 064028 (2017)
12 S. Aneesh, S. Bose, and S. Kar, Phys. Rev. D, **97**: 124004 (2018)
13 B. P. Abbott et al (LIGO Scientific Collaboration and Virgo Collaboration), Phys. Rev. Lett., **116**: 061102 (2016)
14 B.P. Abbott et al (LIGO Scientific Collaboration and Virgo Collaboration), Phys. Rev. Lett., **119**: 161101 (2017)
15 A. Krolak and M. Patil, Universe, **3**: 59 (2017)
16 N. Stergioulas, Living Rev Relativ., **1**: 8 (1998)
17 J. Abadie et al (LIGO Scientific Collaboration), Nat. Phys., **7**: 962 (2011)
18 M. Page, J. Qin, J. La Fontaine, C. Zhao, and D. Blair, Phys. Rev. D, **97**: 124060 (2018)
19 P. A. Gonzalez, J. Saavedra, and Y. Vasquez, Int. J. Mod. Phys. D, **21**: 125005 (2012)
20 S. Iyer and C. M. Will, Phys. Rev. D, **35**: 3621 (1987)
21 R. A. Konoplya, Phys. Rev. D, **68**: 024018 (2003)
22 R. Konoplya, Phys. Rev. D, **71**: 024038 (2005)
23 R. A. Konoplya and A. Zhidenko, Phys. Rev. Lett., **103**: 161101 (2009)
24 S. Fernando, Phys. Rev. D, **77**: 124005 (2008)
25 S. Fernando, Gen. Rel. Grav., **36**: 71 (2004)
26 S. Fernando, Int. J. Mod. Phys. D, **24**: 1550104 (2015)
27 N. Breton, T. Clark, and S. Fernando, Int. J. Mod. Phys. D, **26**(10): 1750112 (2017)
28 I. Sakalli, Mod. Phys. Lett. A, **28**: 1350109 (2013)
29 I. Sakalli and S. F. Mirekhtiary, Astrophys.Space Sci., **350**: 727 (2014)
30 I. Sakalli, Eur. Phys. J. C, **75**(4): 144 (2015)
31 B. S. Kandemir and U. Ertem, Annalen Der Physik, **529**: 1600330 (2017)
32 I. Sakalli and G. Tokgoz, Annalen Der Physik, **528**: 612 (2016)
33 A. Övgün and K. Jusufi, Annals Phys. **395**: 138 (2018)
34 I. Sakalli, K. Jusufi, and A. Övgün, arXiv:1803.10583 [gr-qc]
35 K. Jusufi, I. Sakalli and A. Övgün, Gen. Rel. Grav., **50**(1): 10 (2018)
36 P. A. Gonzalez, A. Övgün, J. Saavedra, and Y. Vasquez, Gen. Rel. Grav., **50**(6): 62 (2018)
37 R. Becar, S. Lepe, and J. Saavedra, Phys.Rev. D, **75**: 084021 (2007)
38 J. Saavedra, Mod. Phys. Lett. A, **21**: 1601 (2006)
39 S. Lepe, and J. Saavedra, Phys. Lett. B, **617**: 174 (2005)
40 J. Crisostomo, Samuel Lepe and J. Saavedra, Class. Quant. Grav. **21**: 2801 (2004)
41 P. A. Gonzalez, E. Papantonopoulos, J. Saavedra, and Y.Vasquez, Phys. Rev. D, **95**(6): 064046 (2017)
42 M. Cruz, M. Gonzalez-Espinoza, J. Saavedra, and D. Vargas-Arancibia, Eur. Phys. J. C, **76**(2): 75 (2016)
43 X. Kuang and J. Wu, Phys. Lett. B, **770**: 117 (2017)
44 X. He, B. Wang, S. Wu, and C. Lin, Phys. Lett. B, **673**: 156 (2009)
45 X. Rao, B. Wang, and G. Yang, Phys. Lett. B, **649**: 472 (2007)
46 S. Chen, B. Wang and R. Su, Class. Quantum Grav., **23**: 7581 (2006)
47 X. He, Songbai-Chen, B. Wang, R. Cai, and C. Lin, Phys. Lett. B, **665**: 392 (2008)
48 X. He, B. Wang, and S. Chen, Phys. Rev. D, **79**: 084005 (2009)

49 B. Wang, C. Lin and E. Abdalla, Phys. Lett. B, **481**: 79 (2000)
50 B. Wang, C. Lin, and C. Molina, Phys. Rev. D, **70**: 064025 (2004)
51 A. Jansen, Eur. Phys. J. Plus, **132**(12): 546 (2017)
52 M. Halilsoy and A. Al-Badawi, IL Nuovo Cimento B, **113**: 761 (1998)
53 M. Halilsoy, Gen. Relativ. Gravit., **25**(3): 275 (1992)
54 M. Halilsoy and A. Al-Badawi, Class. Quantum Grav., **12**: 3013 (1995)
55 A. Ovgun, Int. J. Theor. Phys., **55**(6): 2919 (2016)
56 H. Reissner, Annalen der Physik (in German), **50**: 106 (1916)
57 G. Nordström, Verhandl. Koninkl. Ned. Akad. Wetenschap., Afdel. Natuurk., Amsterdam., **26**: 1201 (1918)
58 S. Chandrasekhar, The Mathematical Theory of Black Holes (New York: Oxford University Press, 1983)
59 R. M. Wald, General Relativity (The University of Chicago Press, Chicago and London, 1984)
60 S. Q. Wu and X. Cai, J. Math. Phys. (N.Y.), **44**: 1084 (2003)
61 M. Abramowitz and I. A. Stegun, Handbook of Mathematical Functions (Dover, New York, 1965)
62 H. S. Vieira, V. B. Bezerra, and G. V. Silva, Ann. Phys. (Amsterdam), **362**: 576 (2015)
63 K. Heun, Math. Ann., **33**: 161 (1888)
64 A. Ronveaux, Heun's differential equations: (New York: Oxford University Press, 1995)
65 R. S. Maier, The 192 Solutions of Heun Equation: (Preprint math CA/0408317, 2004)
66 P. P. Fiziev, J. Phys. A: Math. Theor., **43**: 035203 (2010)
67 I. Sakalli and M. Halilsoy, Phys. Rev. D, **69**: 124012 (2004)
68 A. Al-Badawi and I. Sakalli, J. Math. Phys., **49**: 052501 (2008)
69 T. Birkandan and M. Hortacsu, EPL, **119**(2): 20002 (2017)
70 I. Sakalli, Phys. Rev. D, **94**: 084040 (2016)
71 G. V. Kraniotis, 2016 Class. Quantum Grav., **33**: 225011 (2016)
72 Here, the computer package, Maple 2017 is used for solving the confluent Heun differential equation
73 H. S. Vieira and V. B. Bezerra, Ann. Phys. (NY), **373**: 28 (2016)
74 H. S. Vieira, J. P. Morais Graca, and V. B. Bezerra, Chin. Phys. C, **41**: 095102 (2017)
75 V. Frolov and I. Novikov, Black Hole Physics: Basic Concepts and New Developments. Fundamental Theories of Physics (Kluwer Academic, London, 1998)
76 P. P. Fiziev, Class. Quantum Grav., **27**: 135001 (2010)
77 S. A. Teukolsky, Phys. Rev. Lett., **29**: 1114 (1972); S. A. Teukolsky, Astrophys. J., **185**: 635 (1973); W. H. Press and S. A. Teukolsky, Astrophys. J., **185**: 649 (1973); S. A. Teukolsky and W. H. Press, Astrophys. J., **193**: 443 (1974)
78 P. P. Fiziev, Phys. Rev. D, **80**: 124001 (2009)
79 S. Chandrasekhar, Proc. R. Soc. London A, **348**: 39 (1976); Proc. R. Soc. London A, **372**: 475 (1980)
80 S. Hod, arXiv:gr-qc/0307060 (2003)
81 E. Berti, V. Cardoso, K. D. Kokkotas, and H. Onozawa, Phys. Rev. D, **68**: 124018 (2003)
82 L. Motl, Ad. Theor. Math. Phys., **6**: 1135 (2002)
83 R. A. Konoplya and A. Zhidenko, Rev. Mod. Phys., **83**: 793 (2011)
84 H. J. Blome and B. Mashhoon, Phys. Lett. A, **110**: 231 (1984)
85 P. Musgrave and K. Lake, Class. Quant. Grav., **13**: 1885 (1996)
86 B. Toshmatov, A. Abdujabbarov, Z. Stuchlik, and B. Ahmedov, Phys. Rev. D, **91**: 083008 (2015)
87 B. Toshmatov, A. Abdujabbarov, J. Schee, and B. Ahmedov, Phys. Rev. D, **93**: 124017 (2016)
88 V. Cardoso, A. S. Miranda, E. Berti, H. Witeck, and V. T. Zanchin, Phys. Rev. D, **79**: 064016 (2009)
89 B. Mashhoon, Phys. Rev. D, **31**: 290 (1985)
90 R. A. Konoplya and Z. Stuchlik, Phys. Lett. B, **771**: 597 (2017)